**Proceedings of the Australian Combustion Symposium**
**November 6-8, 2013, The University of Western Australia**

# Numerical Study of Oxygen Dilution and Temperature Distribution of Biogas Combustion in Bluff-Body MILD Burner

M.M. Noor[1,2,*], Andrew P. Wandel[1] and Talal Yusaf[3]

[1]Computational Eng. and Science Research Centre, School of Mech. and Elec. Engineering, USQ, Australia
[2]Faculty of Mechanical Eng., Universiti Malaysia Pahang (UMP), Malaysia
[3]National Centre for Engineering in Agriculture, University of Southern Queensland (USQ), Australia

**Abstract:** Cleaner and more efficient combustion processes are demanded by the combustion industry due to fuel depletion and air quality issues. A numerical study of a laboratory scale combustor is reported. The numerical simulations were carried out using ANSYS Fluent 14.5. Turbulence was modelled using the realizable k–ε model. The combustion chamber is an open end cylinder with the burner mounted at the bottom of the combustor. Biogas was used as a fuel with 60% methane and 40% carbon dioxide and oxidiser used was atmospheric air and synthetic air by mixing oxygen and nitrogen. The oxygen dilution ratio was analysed at the exhaust gas recirculation (EGR) and air supply mixing area. The dilution ratio is 40% for atmospheric air and a lower ratio when the low-oxygen synthetic air was used. The temperature throughout the combustion chamber was found to be close to homogeneous. The inlet air velocity did not affect the chamber and EGR temperature. In these simulations, MILD combustion was achieved.
*Keywords: computational fluid dynamics, bluff-body MILD burner, biogas*

## 1. Introduction

Clean energy production with lower emissions and higher efficiencies is becoming a global demand [1-3]. One of the new combustion technologies to reduce combustion pollution emission with higher thermal efficiency is moderate or intense low oxygen dilution (MILD) combustion [4-7] or flameless oxidation (FLOX) [8-9]. The desire to improve the efficiency with lower emissions has led to an increased interest in combustion modeling [10-11]. By using biogas [12-14] or low calorific value (LCV) gas, $CO_2$ emitted by the combustion will be utilized by biomass, which is the source of biogas. In this study, LCV gas was produced by mixing methane and carbon dioxide. The purpose of this study is to analyze the chamber temperature and the oxygen dilution by exhaust gas recirculation (EGR).

## 2. CFD Modeling

Computational Fluid Dynamics (CFD) modeling has been successful in numerically solving many engineering problems [15-19]. Many researchers have successfully used numerical simulation to study MILD and flameless combustion [20-23]. The open furnace geometry is shown in Fig. 1, which will be used in the simulation work using FLUENT 14.5. The overall dimension is 2.0 m high and 0.6 m wide. Detail on the model setup is shown in Table 1. A bluff body burner was used to mix the streams, with the fuel nozzle (1 mm in diameter) located at the center of the burner and fuel inlet directly under the fuel nozzle with inlet diameter of 10 mm . With a fuel injection velocity of 1 m/s, the volume flow rate for the fuel was $7.85\text{x}10^{-5}$ $m^3/s$. The air nozzle into the combustion chamber was a 10 mm radius annulus with 392.5 $mm^2$ opening fed by 4 inlets that inject into each EGR pipe. Each air inlet diameter was 10 mm for a total of 314 $mm^2$. The air-fuel ratio used in this study was 4.4:1 [24]. The method of meshing was tetrahedrons (patch conforming) with advanced sizing function of proximity and curvature; detail settings for the modeling are reported elsewhere [25]. The mesh inflation for the near the wall was 5 layer with growth rate of 20%. Mesh element refinement was used at air, fuel inlet, air fuel nozzle and EGR inlet and outlet. The total number of mesh elements and nodes generated from the geometry was 687,940 and 247,254 respectively. Figure 2 shows the mesh element from front view of the burner. The grid independence study was reported in [26].

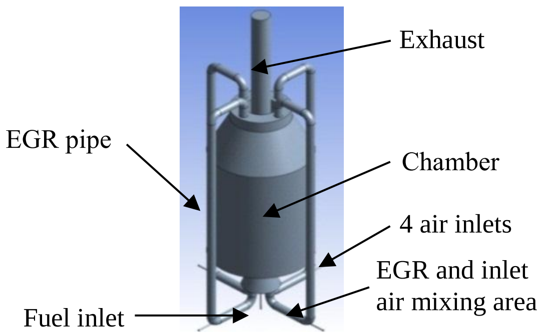


Figure 1: Open furnace geometry with boundary conditions

Table 1: Typical data for burner and combustion chamber

| Item | Data |
|---|---|
| Fuel | 60% methane and 40% carbon dioxide |
| Oxidizers | Atmospheric and synthetic air at room temperature |
| Fuel / Air Inlet | 1 x 78.5 $mm^2$ / 4 x 78.5 $mm^2$ |
| Chamber size | Diameter 600mm, Height 860mm |
| EGR | 4 EGR with 1962.5 $mm^2$ each inlet |

The maximum Skewness was 0.8827, below the allowable limit of 0.9800, which is necessary to prevent divergence errors in the solution and allow satisfactory converge [24]. The simulation of MILD combustion involved the solution of the chemical reactions, turbulent flows, heat transfer and species transport. The chemical

* Corresponding author:
Phone: (+61) 7 4631 1758
Email: muhamad@ump.edu.my

reactions were modelled by considering chemical equilibrium based on the mixture fraction with non-adiabatic energy treatment. In this work, the Reynolds–Averaged Navier–Stokes (RANS) equations together with the realizable k-ε turbulence model [27] were solved. The discrete ordinate (DO) radiation model [28] and absorption coefficient of weighted sum of gray gas (WSGGM) model was used.

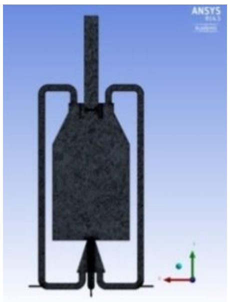

Figure 2: Model after meshing

The fuel for this study was biogas, which is a LCV gas. The biogas was produced by mixing 60% methane and 40% carbon dioxide. The parameters studied were air and fuel inlet velocity, exhaust opening and air inlet oxygen mole fraction content. For exhaust opening, the parameters selected were 5% opening which was nearly fully closed and 95% opening which was nearly fully open. Tables 2 and 3 show the parameters for the air and fuel inlet velocity and oxygen mole fraction.

Table 2: Air and fuel inlet velocity for oxygen mole fraction

| Air Inlet (m/s) | Fuel inlet (m/s) for air oxygen mole fraction of | |
|---|---|---|
| | 7% | 21% |
| 7 | 2.1 | 6.4 |
| 8 | 2.4 | 7.3 |
| 9 | 2.7 | 8.2 |
| 10 | 3.0 | 9.1 |
| 15 | 4.5 | 13.6 |

Table 3: Oxygen mole fraction and fuel velocity for 10m/s air inlet

| Air oxygen mole fraction (%) | 3 | 7 | 11 | 15 | 19 | 21 | 23 |
|---|---|---|---|---|---|---|---|
| Fuel Inlet (m/s) | 1.3 | 3.0 | 4.8 | 6.8 | 8.2 | 9.1 | 10 |

The aim of this study was to investigate the phenomena of MILD combustion using open chambers with EGR; the current study investigates the behavior with low and high amounts of EGR. Besides the chamber maximum and average temperature, the temperature after the air and EGR have mixed also reported. The oxygen dilution and the oxidant temperature are the important parameters to achieve the MILD regime. Therefore the oxygen dilution was measured in this study.

## 3. Results and Discussions

The results of the simulations are discussed below.

### 3.1 Temperature measurement

The simulation results for the temperature distributions are shown in Figs. 3–7. The temperature contours for synthetic air with 7% oxygen and atmospheric air are compared in Fig. 3. The chamber average temperature for the combustion of biogas with synthetic air with reduced oxygen mole fraction is lower (842K) compared to the normal oxygen level (1175K). Figure 4 shows the combustion chamber contour of temperatures for exhaust opening of 95%. The majority of both domains are close to the average temperature of the combustion chamber: for synthetic air with 7% oxygen, the displayed temperature range is 820K to 870K and for the atmospheric air, temperature range is 1160K to 1220K.

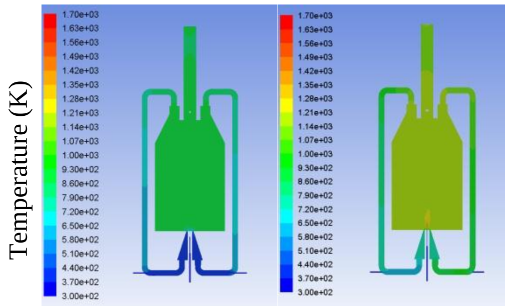


Figure 3: Chamber temperature distribution for the exhaust opening of 95% on the synthetic air with 7% oxygen (left) and atmospheric air (right).

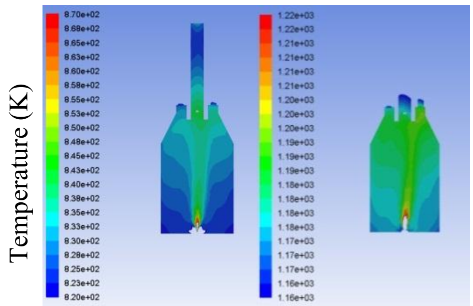


Figure 4: Chamber temperature distribution for 95% exhaust opening, synthetic air with 7% oxygen (left) showing 820–870K and atmospheric air (right) showing 1160–1220K

Figure 5 shows the equivalent results to Fig. 4 for exhaust openings of 5%. The majority of both domains are close to the average temperature of the combustion chamber: for synthetic air with 7% oxygen, the displayed temperature range is 825K to 870K and for the atmospheric air, temperature range is 1150K to 1230K.

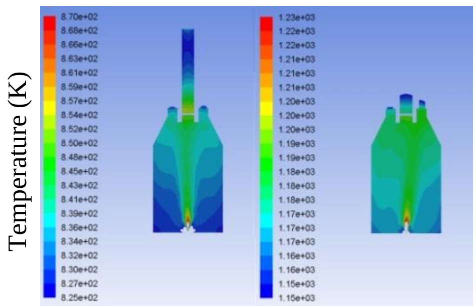


Figure 5: Chamber temperature distribution for 5% exhaust opening, synthetic air with 7% oxygen (left), range from 825K to 870K and atmospheric air (right), range from 1150K to 1230K

This result signifies that the chamber average temperature is identical for both 5% and 95% exhaust opening, so the EGR is effective even for small amounts. The temperature distribution with small range proves that the MILD combustion was achieved for the simulation for both synthetic and atmospheric air. The temperature distributions for both Figs. 4 and 5 show that the hottest zone is slightly above the fuel nozzle where the streams first mixed. The maximum chamber temperature is shown in Fig. 6. Maximum and average temperature inside the chamber and air mixing temperature is plotted in Figs. 7 and 8. The exhaust opening of 5% and 95% do not affect the chamber temperature. The average chamber temperature for both cases is below 1300K.

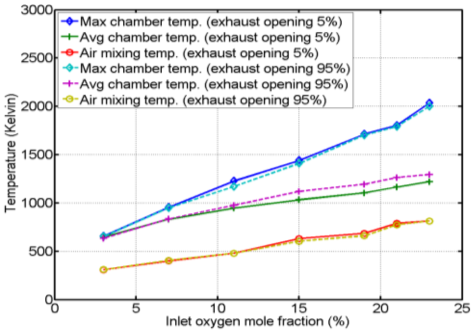


Figure 6: Maximum and average chamber and mixing temperatures. Exhaust opening 5%, –; Exhaust opening 95%, --.

Figure 7 shows the maximum and average chamber temperature and air mixing temperature for differences air inlet velocity. From the result, it shows that the air inlet velocity has negligible effect on the temperature.

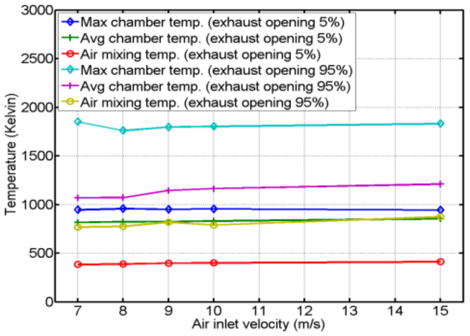


Figure 7: Effect of air inlet velocity to chamber and mixing temperatures

## 3.2 Oxygen dilution

Oxygen dilution is very important to achieve the MILD combustion regime: oxygen mole fraction must be in the range of 3-13% [6,29]. Oxygen dilution can be measured by the dilution ratio ($K_v$). Wünning and Wünning [30] calculated the dilution ratio $K_V$ with EGR as:

$$K_V = \frac{M_{EGR}}{(M_A + M_F)} = \frac{(M_T - M_A - M_F)}{(M_A + M_F)} \qquad (1)$$

The total mass flow rate ($M_T$) is calculated by adding up the EGR mass flow rate ($M_{EGR}$), fuel mass flow rate ($M_F$) and fresh air mass flow rate ($M_A$). The equivalence of mass and volume flow rates is for constant-density processes. Figure 8 shows the oxygen mole fraction at air inlet and oxygen mole fraction dilution after the inlet air has mixed with the EGR: this is the oxidizer stream in the combustion chamber.

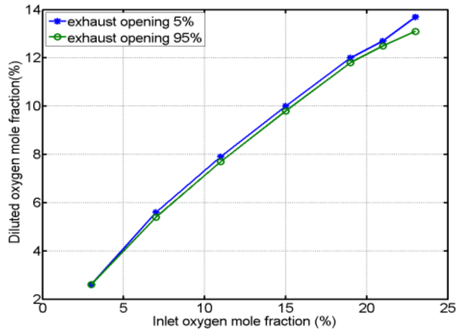


Figure 8: Oxygen mole fraction for inlet oxidant (x-axis) and diluted oxidant that entering combustion chamber (y-axis).

There are only small differences between the exhaust openings of 5% and 95%. Figure 9 shows the ratio of the inlet oxidant that is diluted by the EGR. The ratio increases monotonically with increase in oxygen mole fraction.

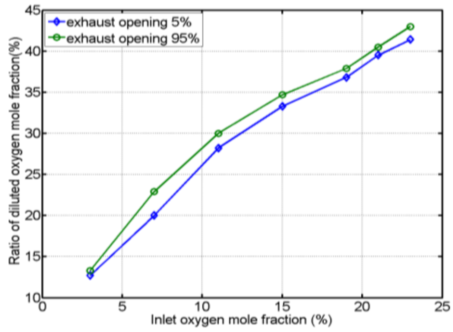


Figure 9: Oxygen mole fraction for inlet oxidant (x-axis) and the ratio of diluted oxidant that entering combustion chamber (y-axis).

Figure 10(left) shows the diluted oxygen mole fraction for synthetic air of 7% oxygen, which is diluted by the EGR to the level of 5.6%. Figure 10(right) shows that the oxygen was consumed in the combustion process.

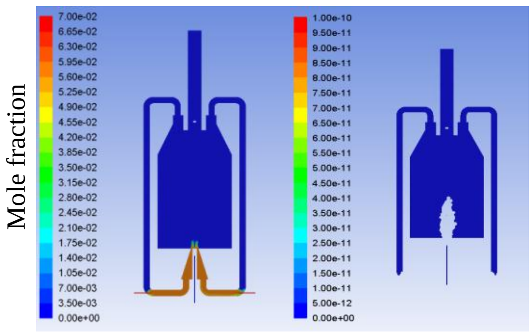


Figure 10: Oxygen mole fraction diluted for synthetic air with 7% oxygen. The mole fraction is shown for the full range of 0 to 7% (left) and the range of 0 to $1x10^{-8}$ % (right).

Similar behaviour is seen for methane (Fig. 11(left)) where 60% of methane mole fraction was consumed in the combustion process; less than 0.75% was unburned (Fig. 11(right)) and released with the exhaust gas.

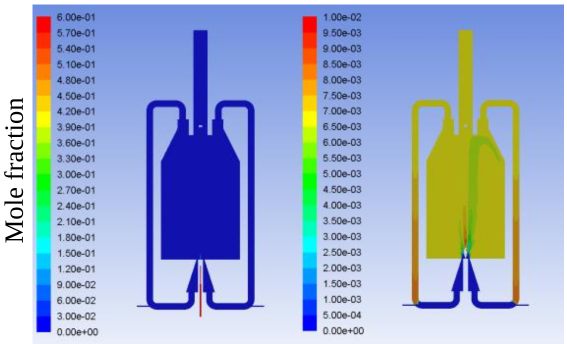


Figure 11: As per Fig. 10 for methane mole fraction with full range of 0 to 60% (left) and the range of 0 to 0.1 % (right).

Figure 12(left) shows CO mole fraction where very low percentage (0.4%) was released as a combustion product. Fig. 12(right) is $CO_2$ mole fraction where 40% was injected through fuel inlet and 7% of $CO_2$ was released together with exhaust gas. Water vapour in combustion product was 6.42% as shown in Fig. 13. If higher air-fuel inlet ratio (6.0:1) was used, water vapour is 6.29% and if lower air-fuel inlet ratio (2:1), water vapour is 6.59%. This is due to the higher fuel inlet producing more water vapour from the combustion process.

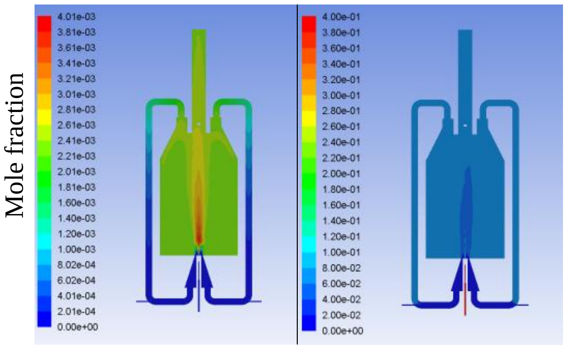


Figure 12: CO and $CO_2$ mole fraction with CO for the range of 0 to 0.4% (left) and $CO_2$ for the range of 0 to 40% (right).

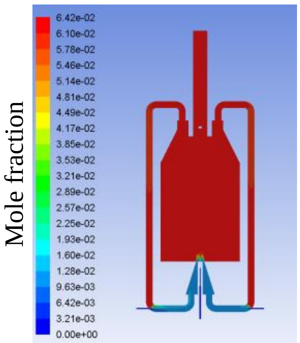


Figure 13: Water vapour mole fraction

These simulation results will be validated by experimental technique as the burner has been manufactured and is about to undergo commissioning, as shown in Fig. 14. More details about the burner design and development can found in [31-32]. It's allow the chamber to operate as a fully open, partially open or nearly closed furnace. This setting will result in different amounts of EGR to dilute the oxidant.

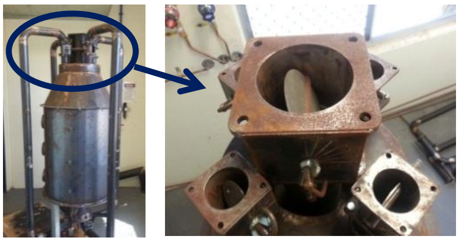

Figure 14: Burner development, whole furnace (left) and damper for exhaust at the top of the burner and EGR pipe (right).

## 4. Conclusion

The flame temperature in MILD combustion regime is studied numerically for non-premixed combustion with chemical equilibrium and non-adiabatic energy treatment using RANS equations and realizable k-ε turbulence model. Of primary interest were the temperature distributions in the chamber and oxygen dilution when mixing fresh air and EGR flue gas. The exhaust settings were 95% open for near fully open chamber and 5% open for near fully close chamber. A few conclusions can be made from the study:

i. The chamber temperature distribution was found to be in a small range: between 820K to 870K for the synthetic air with 7% oxygen and between 1150K to 1230K for normal atmospheric air.
ii. The chamber temperature distributions are identical for both 5% and 95% exhaust opening.
iii. Air inlet velocity has no effect on the chamber and air mixing temperatures.
iv. The oxygen diluted ratio for atmospheric air is about 40% and the oxygen mole fraction reduces from 21% to 12.6%. This is below 13% as a requirement to achieve MILD combustion.
v. The numerical analysis has met the purpose of the study with the chamber's temperature distribution showing that MILD combustion was achieved as required.

## 5. Acknowledgments

Thanks to USQ, MOE, Malaysia and UMP for providing financial support and laboratory facilities.

## 6. References

[1] IEA, World Energy Outlook, (2006), Paris
[2] Orr F, Energy and Climate, GCEP. (2005) Stanford Uni.
[3] IEA, Org. for Economic Co-Opr. Dev., (2009), Paris
[4] Cavaliere A and Joannon MD, PECS, 30 (2004) 329-366.
[5] Christo FC and Dally BB 15th Australasian Fluid Mech. Conf., Uni. of Sydney, Australia, 2004, p. 1-4.
[6] Noor MM, Wandel AP and Yusaf IJAME, 6(2012) 730-754.
[7] Joannon MD, Langella G, Beretta F, Cavaliere A and Noviella C, Comb. Sc. and Tech. 153(1) (2000) 33-50.
[8] Wünning JA, CI-Tech. 63(12) (1991) 1243-1245.
[9] Wünning JG, PhD Thesis, (1996), Aachen
[10] Smith ST and Fox RO, Phy. of Fluids, (2007), 19:085102.
[11] Merci B, Naud B and Roekaerts D, FTC, 79 (2007) 41-53.
[12] Colorado, AF, Medwell, PR and Dally, BB. Australian Comb. Sym., UQ, Australia, 2-4 Dec 2009, p. 1-4.
[13] Dally BB, Shim SH, Craig RA, Ashman PJ and Szego GG, Energy and Fuels, 24 (2010) 3462-3470.

[14] Colorado AF, Herrera BA and Amell AA Bioresource Tech. 101(7) (2010) 2443-2449.
[15] Dally BB, Fletcher DF and Masri AR 1998 Comb. Theory and Mod. 2 (1998) 193-219.
[16] Wandel AP, Smith NSA and Klimenko AY Int. Conf. on CFD, Springer-Verlag, 2003, p. 789-790.
[17] Najiha MA, Rahman MM, Kamal M, Yusoff AR and Kadirgama K, J. of Mech. Eng. and Sc. 3(2012), 340-345
[18] Rahimi M, Khoshhal A and Shariati SM, App. Thermal Eng. 26(2006) 2192-2200.
[19] Rahim R, Mamat R and Taib MY NCMER2010, 3-4 Dec, Malaysia, 2010 pp. 863-870
[20] Parente A, Galletti C, Tognotti L, Int. J. Hyd. Energy, 33 (2008) 7553 -7564.
[21] Noor MM, Wandel AP and Yusaf T, Int. Conf. of Mech. Eng. Res.,1-3 Jul, Malaysia, 2013, ICMER2013-P245
[22] Galletti C, Parente, A, Tognotti L, CF, 151 (2007) 649-664.
[23] Mardani A, Tabejamaat, S, Ghamari, M, Comb. Theory and Mod., 14 (2010) 747-774.
[24] Noor MM, Wandel AP and Yusaf T, Malaysian PG Conf., 4-5 Jul, Australia, 2013, MPC2013-08.
[25] Noor MM, Wandel AP and Yusaf T, Int. Conf. of Mech. Eng. Res.,1-3 Jul, Malaysia, 2013, ICMER2013-P342.
[26] Noor MM, Wandel AP and Yusaf T, J. of Mech. Eng. and Sc., (2013) (Accepted).
[27] Shih TH, Liou, WW, Shabbir, A, Yang, Z and Zhu J. Computers and Fluids 24(3) (1995) 227-238.
[28] Chui EH and Raithby GD, NHTB 23(3) (1993) 269-288.
[29] Li PF, Mi JC, Dally BB, Wang FF, Wang L, Liu ZH, Chen S and Zheng CG, China T Sc., 54 (2011) 255-269.
[30] Wünning JA and Wünning JG PECS, 23(1) (1997) 81-94.
[31] Noor MM, Wandel AP and Yusaf T, Int. Conf. of Mech. Eng. Res.,1-3 Jul, Malaysia, ICMER2013-P341.
[32] Yusaf T, Noor MM and Wandel AP, Int. Conf. of Mech. Eng. Res., 1-3 Jul, Malaysia, ICMER2013-K03.